NUMERICAL PERFORMANCE STUDY OF PARAFFIN WAX DISPERSED WITH ALUMINA IN A CONCENTRIC PIPE LATENT HEAT STORAGE SYSTEM

by

Amirtham VALAN ARASU [a]*, Agus P. SASMITO [b], and Arun S. MUJUMDAR [b]

[a] Department of Mechanical Engineering, Thiagarajar College of Engineering, Madurai, Tamil Nadu, India
[b] Department of Mechanical Engineering, National University of Singapore, Crescent, Singapore, Singapore

Original scientific paper
DOI: 10.2298/TSCI110417004A

Latent heat energy storage systems using paraffin wax could have lower heat transfer rates during melting/freezing processes due to its inherent low thermal conductivity. The thermal conductivity of paraffin wax can be enhanced by employing high conductivity materials such as alumina (Al_2O_3). A numerical analysis has been carried out to study the performance enhancement of paraffin wax with nano-alumina (Al_2O_3) particles in comparison with simple paraffin wax in a concentric double pipe heat exchanger. Numerical analysis indicates that the charge-discharge rates of thermal energy can be greatly enhanced using paraffin wax with alumina as compared with a simple paraffin wax as phase change materials.

Key words: *latent heat storage system, phase change material, paraffin wax, paraffin wax with Al_2O_3, concentric pipe heat exchanger, melting-freezing cycle*

Introduction

Energy storage not only reduces the mismatch between supply and demand but also improves the performance and reliability of energy systems. Thermal energy can be stored in the form of sensible heat in which the energy is stored by raising the temperature of the storage material solid or liquid. Rock or water is the best example. Alternatively, thermal energy can be stored as latent heat in which energy is stored when a substance changes from one phase to another by either melting or freezing. The temperature of the substance remains constant during phase change. Of the two, latent heat thermal energy storage technique has proved to be a better engineering option primarily due to its advantage of providing higher energy storage density with a smaller temperature difference between storage and retrieval. Phase change materials (PCM) are materials that use chemical bonds to store and release heat energy in the process of changing the state from solid to liquid.

Among the variety of PCM proposed, paraffin wax has been considered most prospective, because of its desirable characteristics, including significant latent heat of fusion, negligible supercooling, low vapor pressure in melt, chemical stability, and 100% recyclable. However, the inherent low thermal conductivity of paraffin could result in lower heat transfer rates during melting/freezing processes. In order to enhance the effective thermal conductivity usually highly conducting materials are added to the paraffin wax either metallic fins connected to the heat exchanging surfaces (or) metal pieces which are not connected to each other.

* Corresponding author; e-mail: a_valanarasu@yahoo.com

The performance of different types of heat exchangers used as latent heat thermal storage (LHTS) units has been investigated by many researchers [1]. Sharma *et al*. [2] have reviewed various kinds of heat exchangers proposed by researchers. Among these shell and tube/concentric double pipe heat exchangers have been proved as high efficient for minimum volume [3, 4].

The thermal conductivity of paraffin wax can also be enhanced by employing high conductivity materials. While unloading a latent heat storage, the solid-liquid interface moves away from the heat transfer surface and the heat flux decreases due to the increasing thermal resistance of the growing layer of the molten/solidified medium. This effect can be reduced using a technique of dispersing high conductivity materials to increase heat transfer. Cabeza *et al*. [5] compared three methods to enhance the heat transfer in a cold storage working with water/ice as PCM: addition of stainless steel pieces, copper pieces, and a new PCM-graphite composite material. The PCM-graphite composite material showed an increase in heat flux bigger than with any of the other techniques.

Mettawee and Assassa [6] conducted experiments to investigate the enhancement in the performance of PCM based solar collector due to the dispersion of micro aluminum particles. Due to increase in thermal conductivity, the charging time was decreased by 60% as compared to that of pure PCM. The effect was more pronounced during discharging, as the conduction dominated solidification presented more homogeneous process.

Khodadadi and Hosseinizadeh [7] have simulated the solidification of nanofluid (water with nano copper particles] in a square storage model. The speed of the solid/liquid interface during solidification was observed for pure PCM and for PCM with different particle mass fractions. At earlier stages there was not much increase in the speed of the interface due to the addition of particles. As the time elapsed the effect was more pronounced as the interface was at more advanced locations in case of higher mass fractions. This resulted in considerable reduction in overall solidification time. Besides copper and aluminum particles, silver [8] and graphite [9, 10] have also been tried to obtain composite PCM.

Alumina (Al_2O_3) is one of the most common and inexpensive nanoparticles used by many researchers in their experimental investigations [11]. Recently, Ho and Gao [12] prepared the nanoparticle-embedded PCM by emulsion technique using non-ionic surfactant to disperse 5 wt.% and 10 wt.%, of alumina (Al_2O_3) nanoparticles in paraffin (n-octadecane) and investigated experimentally its effective thermophysical properties, including latent heat of fusion, density, dynamic viscosity, and thermal conductivity. They found that the relative increases of nearly 20% and more than 28% in the dynamic viscosity were found for the paraffin containing 5 wt.% and 10 wt.% of alumina particles, respectively at a temperature of 30 °C; which appear far greater than (about ten and four times, respectively) the relative enhancement in the thermal conductivity if compared at the same nanoparticle mass fraction.

Gong and Mujumdar [13-16] have carried out a series of numerical studies on heat transfer during melting and freezing of single and multiple PCM. They extended their analysis from only the charge process (melting) to a combined charge/discharge (melting/ freezing) process [14]. According to Hasan *et al*. [17], if the PCM melts and freezes completely in each period at the periodic steady-state (PSS), the energy stored or released is within 5% of the PSS value in two cycles starting from a uniform temperature for liquid or solid. On the other hand, if there is an active zone at the PSS, the number of cycles required to approach the PSS depends upon the initial phase of a uniform temperature PCM. If the initial phase of the PCM is opposite to that of the PCM beyond the active zone at the PSS, 4 to 6 cycles are required for the energy stored or released to approach within 5% of the PSS value.

In the present work, a numerical analysis has been carried out to investigate the performance enhancement due to the addition of nanoalumina (Al_2O_3) particles in paraffin wax in a concentric double pipe heat exchanger by both the cyclic as well as individual charging and discharging processes for various concentrations of alumina particles and the results are presented and discussed.

Mathematical model

The physical model consists of an inner pipe of 2 cm diameter, through which a heat transfer fluid (HTF) flows. It is surrounded by a concentric pipe of 4 cm diameter consisting of the PCM (fig.1). Following are the two cases for which the numerical study of melting and solidification is carried out and compared: (1) pure paraffin wax and (2) nanoparaffin wax (paraffin wax with 5 vol.% and 10 vol.% Al_2O_3).

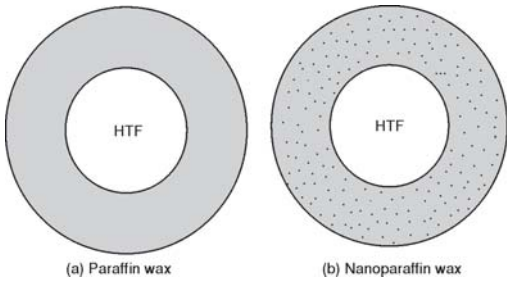

Figure 1. Physical model

In the present work, paraffin wax and paraffin wax with alumina (nanoparaffin wax) are used as PCM. The inner wall of the PCM pipe is maintained at constant temperature of T_{max} = = 350 K during the melting or charging period and at constant temperature of T_{min} = 300 K during the solidification or discharging period. The outer wall of the PCM pipe is adiabatic.

For a mathematical description of the thermal process the following assumptions are made:

– the inner wall is at a constant temperature,
– thermal losses through the outer wall of the PCM pipe are negligible,
– thermal resistance of the inner pipe wall is negligible,
– heat transfer in the PCM is both conduction and convection controlled,
– thermophysical properties of PCM are temperature dependent, and
– volume variation resulting from the phase change is neglected and the PCM solid is fixed to the walls at all times.

An enthalpy-porosity technique is used in FLUENT for modelling the solidification/melting process. In this technique, the liquid melt fraction in each cell is computed every iteration, based on enthalpy balance. The mushy zone is the region where the porosity increases from 0 to 1 as the PCM melts. When the region is complete solid, the porosity is zero and also the flow velocity in that zone also drops to zero.

The governing conservation equations are [18]:

– *continuity equation*

$$\frac{\partial \rho}{\partial t} + \nabla(\rho \vec{\mathrm{U}}) = 0 \tag{1}$$

– *momentum equation*

$$\frac{\partial}{\partial t}(\rho \vec{\mathrm{U}}) + \nabla(\rho \vec{\mathrm{U}} \vec{\mathrm{U}}) = -\nabla P + \rho \vec{\mathrm{g}} + \nabla \boldsymbol{\tau} + \vec{\mathrm{F}} \tag{2}$$

where P is the static pressure, $\boldsymbol{\tau}$ – the stress tensor, and $\rho \vec{\mathrm{g}}$ and $\vec{\mathrm{F}}$ are the gravitational body force and external body forces, respectively,

– *energy equation*

$$\frac{\partial(\rho H)}{\partial t} + \nabla(\rho \vec{\mathrm{U}} H) = \nabla(K \nabla T) + S \tag{3}$$

where H is the enthalpy of the PCM, T – the temperature, ρ – the density of the PCM, K – the thermal conductivity of PCM, $\vec{U}$ – the velocity, and S – the volumetric heat source term and is equal to zero in the present study. The total enthalpy H of the material is computed as the sum of the sensible enthalpy, h and the latent heat:

$$H = h + \Delta H \tag{4}$$

where

$$h = h_{\text{ref}} + \int_{T_{ref}}^{T} c_p \mathrm{d}T \tag{5}$$

and h_{ref} is the reference enthalpy, T_{ref} – the reference temperature, and c_p – the specific heat at constant pressure.

The latent heat content, in terms of the latent heat of the PCM, L is:

$$\Delta H = \beta L \tag{6}$$

where β is the liquid fraction and is defined as:

$$\begin{aligned} &\beta = 0 && \text{if } T < T_{\text{solidus}} \\ &\beta = 1 && \text{if } T > T_{\text{liquidus}} \\ &\beta = \frac{T - T_{\text{solidus}}}{T_{\text{liquidus}} - T_{\text{solidus}}} && \text{if } T_{\text{solidus}} < T < T_{\text{liquidus}} \end{aligned} \tag{7}$$

The solution for temperature is essentially iteration between the energy, eq. (3), and the liquid fraction, eq. (7).

The enthalpy-porosity technique treats the mushy region (partially solidified region) as a porous medium. The porosity in each cell is set equal to the liquid fraction in that cell. In fully solidified regions, the porosity is equal to zero, which extinguishes the velocities in these regions. The momentum sink due to the reduced porosity in the mushy zone takes the following form:

$$= \frac{(1-\beta)^2}{(\beta^3 + 0.001)} A_{\text{mush}} \vec{U} \tag{8}$$

where A_{mush} is the so called mushy zone constant. The value of mushy zone constant varies from 10^4 to 10^7. Generally, 10^5 is used for FLUENT computations:

– *boundary and initial conditions*

PCM pipe inner wall – charging: $T = T_{\max}$, discharging: $T = T_{\min}$,

PCM pipe outer wall – $K_{\text{npcm}} \Delta T = 0$

– *initial condition*

For cyclic process – $T_{\text{i}} = T_{\min}$

For complete melting and solidification processes – charging: $T_i = T_{\min}$,, discharging: $T_i = T_{\max}$

Computational methodology

The model for the numerical study was created using pre-processor software GAMBIT 2.3.16. Meshing of the numerical model was generated and the boundaries were applied at appropriate surfaces. After mesh independence study, the computational domain was resolved with 1900 elements: a fine structured mesh near the inner wall to resolve the boundary layer and an increasingly coarser mesh in the rest of the domain in order to reduce the computational time. As an indication of the computational time, it is observed that on an average, for

3000 iterations, 120-180 minutes are needed for convergence criteria for all relative residuals with a time step of 0.01s using a personal computer with a Intel Core 2 duo processor (2.1 GHz) and 2 GB random access memory (RAM).

The GAMBIT model is then exported to FLUENT for problem solving. The PRESSURE BASED method within version 6.3.26 of the commercial code FLUENT was utilized for solving the governing equations. User-defined functions (UDF) were written in C language to account for temperature-dependence of the thermo-physical properties of paraffin wax without or with nanoalumina particles. The time step for integrating the temporal derivatives was set to 0.01 s. The FIRST ORDER UPWIND differencing scheme was used for solving the momentum and energy equations, whereas the PRESTO scheme was adopted for the pressure correction equation. The under-relaxation factors for the velocity components, pressure correction and thermal energy were 0.5, 0.3, and 1, respectively. The convergence criteria are set as 10^{-3} for continuity and momentum, and 10^{-6} for thermal energy.

Thermophysical properties

The thermophysical properties of paraffin wax [19] and Al_2O_3 [20], listed in tab. 1 are used in the present numerical study. The difference in the solidus and liquidus temperatures defines the transition from solid to liquid phases during the melting of paraffin wax.

Table 1. Properties of paraffin wax [19] and Al_2O_3 [20]

Property	Paraffin wax	Al_2O_3
Density, ρ [kgm^{-3}]	$\dfrac{750}{0.001(T-319.15)+1}$	3600
Specific heat capacity, c_p [Jkg^{-1}K^{-1}]	2890	765
Thermal conductivity, K [Wm^{-1}K^{-1}]	0.21 if $T < T_{\text{solidus}}$ 0.12 if $T > T_{\text{liquidus}}$	36
Viscosity, μ [Nsm^{-2}]	$0.001\exp\left(-4.25+\dfrac{1790}{T}\right)$	–
Latent heat, L [Jkg^{-1}]	173400	–
Solidus temperature, [K]	319	–
Liquidus temperature, [K]	321	–

The density, specific heat capacity, and latent heat of the nanoPCM are defined as [21]:

$$\rho_{\text{npcm}} = \phi\rho_{\text{np}} + (1-\phi)\rho_{\text{pcm}} \tag{9}$$

$$c_{p,\text{npcm}} = \frac{\phi(\rho c_p)_{\text{np}} + (1-\phi)(\rho c_p)_{pcm}}{\rho_{\text{npcm}}} \tag{10}$$

$$L_{\text{npcm}} = \frac{(1-\phi)(\rho L)_{\text{pcm}}}{\rho_{\text{npcm}}} \tag{11}$$

The dynamic viscosity and thermal conductivity of the nanoPCM are given by [22]:

$$\mu_{\text{npcm}} = 0.983\text{e}^{12.959\phi}\mu_{\text{pcm}} \tag{12}$$

The effective thermal conductivity of the nanoPCM, which includes the effects of particle size, particle volume fraction, and temperature dependence as well as properties of the base PCM and the particle subject to Brownian motion is given by:

$$K_{\text{npcm}} = \frac{K_{\text{np}} + 2K_{\text{pcm}} - 2(K_{\text{pcm}} - K_{\text{np}})\phi}{K_{\text{np}} + 2K_{\text{pcm}} + 2(K_{\text{pcm}} - K_{\text{np}})\phi} K_{\text{pcm}} + 5\cdot 10^4 \beta_{\text{k}} \zeta \phi \rho_{\text{pcm}} c_{p,\text{pcm}} \sqrt{\frac{BT}{\rho_{\text{np}} \text{d}_{\text{np}}}} \text{f}(T,\phi) \quad (13)$$

where B is the Boltzmann constant, $1.381\cdot 10^{-23}$ J/K and

$$\beta_{\text{k}} = 8.4407(100\phi)^{-1.07304} \quad (14)$$

$$\text{f}(T,\phi) = (2.8217\cdot 10^{-2}\phi + 3.917\cdot 10^{-3})\frac{T}{T_{\text{ref}}} + (-3.0669\cdot 10^{-2}\phi - 3.91123\cdot 10^{-3}) \quad (15)$$

where T_{ref} is the reference temperature of 273 K.

The first part of eq. (13) is obtained directly from the Maxwell model while the second part accounts for Brownian motion, which causes the temperature dependence of the effective thermal conductivity. Note that there is a correction factor, ζ in the Brownian motion term, since

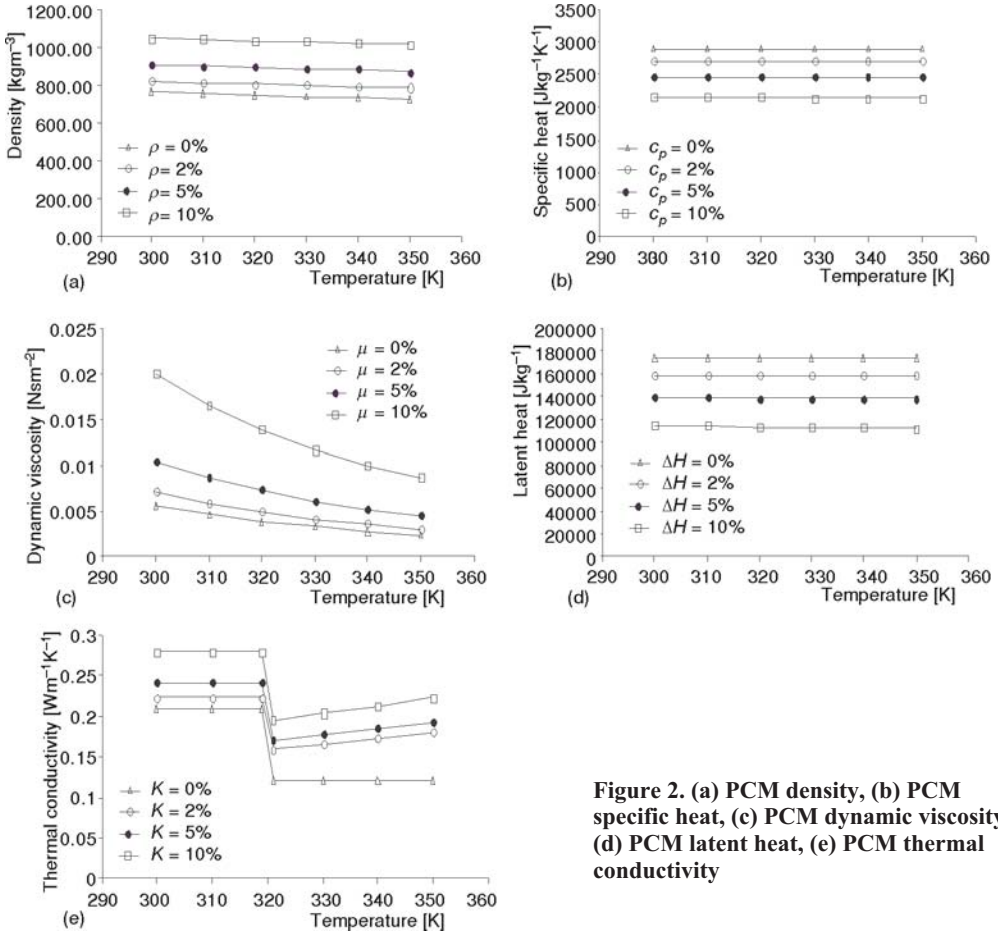

Figure 2. (a) PCM density, (b) PCM specific heat, (c) PCM dynamic viscosity, (d) PCM latent heat, (e) PCM thermal conductivity

there should be no Brownian motion in the solid phase. Its value is defined as the same as for liquid fraction, β, in eq. (7).

The computed thermophysical properties of paraffin wax dispersed with 0%, 2%, 5%, and 10% of Al_2O_3 by volume (nanoPCM) using eqs. (9)-(15) are plotted as a function of temperature and volumetric concentration in figs. 2(a) to 2(e). The specific heat and latent heat of nanoPCM is lower than the simple PCM (paraffin wax) (figs. 2b and 2d) where as the thermal conductivity of nanoPCM is greater than the simple PCM (fig. 2e). Hence, nanoPCM has lower energy storage capacity and higher heart transfer rate compared to the same mass of simple PCM. As shown in fig. 2c, viscosity of nanoPCM increases with the increase in the volumetric concentration of alumina nanoparticles. The enhancement in the dynamic viscosity for the nanoPCM may play a key role in the natural convection dominated melting of nanoPCM. The variation in thermal conductivity and dynamic viscosity of nanoPCM with temperature and volume fraction agree well with the experimental results reported in [12].

Results and discussion

Numerical simulation is carried out for cyclic melting and solidification as well as individual melting and solidification processes of paraffin wax and paraffin wax dispersed with nanoalumina particles and the results are presented and discussed in this section.

Cyclic charge – discharge processes

In order to investigate the advantage of nanoPCM over a simple PCM, the cyclic heat transfer processes of energy charge-discharge using a nanoPCM (with 5% of Al_2O_3) and a simple PCM are simulated for the concentric double pipe heat exchanger system. A cycle consists of one melting process followed by one solidification process.

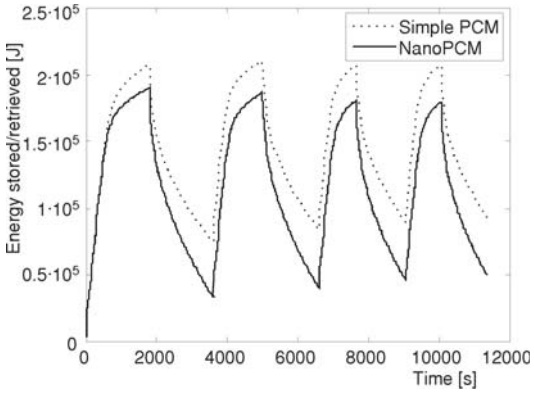

Figure 3. Melting – solidification cycles

At the start of the first cycle, the temperature of the PCM pipe inner wall is maintained at a fixed temperature of 350 K and the PCM is at 300 K. In the extraction period, the PCM pipe inner wall is maintained at a constant temperature of 300 K. In the second and subsequent cycles the operating conditions are repeated identically to the first cycle, except for the time of the charge-discharge period. Simulations are carried out until a steady reproducible state (SRS) or a PSS is reached (fig. 3). In this state, the transient thermal process occurs repeatedly from cycle to cycle and the temperature field in both the PCM and the fluid, as well as the cumulative energy charged-discharged in each charge or discharge period, is the same from cycle to cycle [14].

The magnitude of the cumulative energy charged or discharged, Q_c, is calculated for each melting or freezing period. This calculation is made by computing the difference between the energy stored in the PCM at the end of each melting or freezing process and the energy stored in the PCM at the beginning of the respective period.

The maximum amount of energy which can be charged or discharged in a melting or freezing period is:

$$Q_{\mathrm{t}} = \sum_{i=1}^{2} m \left(\int_{T_{\mathrm{min.}}}^{T_m} c_{\mathrm{p,s}} \mathrm{d}T + L + \int_{T_m}^{T_{\mathrm{max.}}} c_{\mathrm{p,l}} \mathrm{d}T \right) \tag{16}$$

where m is the mass of PCM, $c_{\mathrm{p,s}}$ – the specific heat of solid PCM, $c_{\mathrm{p,l}}$ – the specific heat of liquid PCM , L – the latent heat of melting or fusion of PCM, T_m – the melting or fusion temperature, $T_{\mathrm{min.}}$ and $T_{\mathrm{max.}}$ – are minimum and maximum temperature of the PCM, respectively.

The mass of PCM is given by:

$$m = \rho\pi(r_o^2 - r_i^2)L_{\mathrm{p}} \tag{17}$$

where ρ is the density of PCM, r_{o} and r_i – are the outer and the inner radius of the PCM pipe respectively, and L_{p} is the unit length of the PCM pipe.

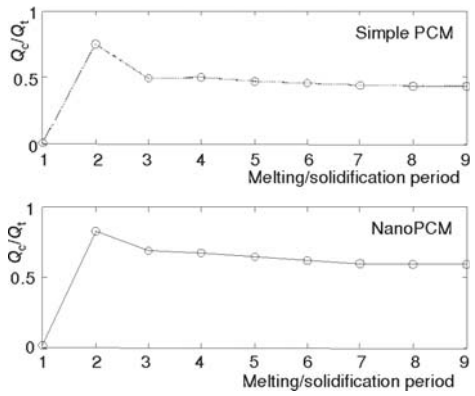

Figure 4. $Q_{\mathrm{c}}/Q_{\mathrm{t}}$ in melting/solidification periods

Figure 4 shows the dimensionless energy stored or recovered, $Q_{\mathrm{c}}/Q_{\mathrm{t}}$, in each melting or freezing period for the PCM. Results are shown for four cycles. In fig. 4 values of $Q_{\mathrm{c}}/Q_{\mathrm{t}}$, each corresponding to the end of either a melting or a solidification period, are joined by straight lines. A cycle constitutes two consecutive values of $Q_{\mathrm{c}}/Q_{\mathrm{t}}$.

A PSS is a state attained when the dimensionless energy stored or recovered in a melting or a solidification period, ($Q_{\mathrm{C}}/Q_{\mathrm{M}}$) is approximately a constant, independent of the initial condition of the PCM. The number of cycles or the time required to approach the PSS depends upon this initial condition. If the PCM is initially a solid, the PSS is reached quickly: however, many more cycles are required if the PCM is initially a liquid [16]. In the present work, the PCM is solid initially and a PSS is attained in the fourth cycle for both cases, but with $Q_{\mathrm{c}}/Q_{\mathrm{t}} = 0.44$ (fig. 4, top) for simple PCM case and $Q_{\mathrm{c}}/Q_{\mathrm{t}} = 0.59$ (fig. 4, bottom) for nanoPCM case.

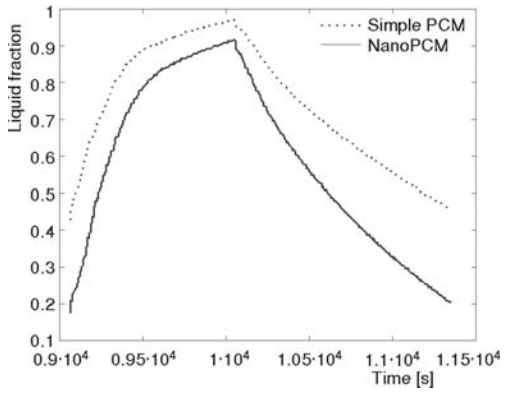

Figure 5. Comparison of liquid fraction during melting and solidification at PSS

The cumulative energy charged-discharged in a charge-discharge cycle at the PSS is 34.1% more when using nanoparaffin wax than that using a simple paraffin wax. This means the energy charge-discharge rates can be 34.1% faster using nanoparaffin wax than using a simple paraffin wax.

Figure 5 shows a comparison of the liquid fractions for a charge-discharge cycle at PSS for the simple and nanoPCM cases. From this figure one can see that with the same temperature for the charge process and for the discharge process, the phase change is much higher for nanoPCM than that in a simple PCM. About 74.4% of the PCM in the nanoparaffin wax is

totally molten at the end of charging and about 71.3% is completely solid at the end of discharging. For simple PCM configuration, about 54.3% of the paraffin wax is molten at the end of charging and 51.4% is completely solid at the end of discharging. So the nanoPCM offers a higher portion of material to undergo a phase change during charging/discharging. This means that more heat is absorbed or released by the nanoPCM than by the simple PCM.

Effect of volumetric concentration of nanoparticles

Time evolution of the melting/solidification rate

The rate of melting or solidification is an important factor in many engineering applications, such as in the LHTS systems. The melting and solidification rate of paraffin wax without or with alumina particles in the concentric double pipe heat exchanger is studied to understand the effect of dispersing the nanoparticles on the performance of the nanoPCM. Figure 6 shows the melting and solidification curves for simple paraffin wax and nanoparaffin wax.

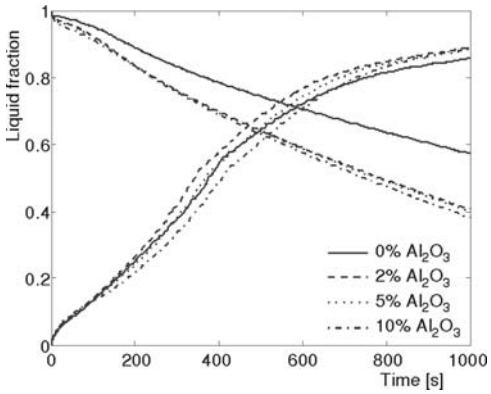

Figure 6. Melting and solidification rate

The melting rate of nanoPCM decreases with the volumetric concentration of Al_2O_3 during the natural convection dominated part of the melting period. The melting performance results obtained in the present simulation study clearly substantiate the doubt concerning the efficacy of dispersing nanoparticles for heat transfer enhancement of the natural-convection-dominated melting process that the enhancement in the thermal conductivity of the nanoPCM due to dispersing the alumina nanoparticles, relative to the simple PCM, could be outweighed by the far greater enhancement in the dynamic viscosity as inferred by Ho and Gao [12].

From fig. 6, it can be seen that the effect of dispersing nanoparticles is much more pronounced in solidification process than in the melting process. Because, solidification process, contrary to melting process, is dominated by conduction. During solidification, the solidified layers are formed from heat transfer surface and remain parallel to it. Although natural convection exists in the liquid PCM at earlier stages, it diminishes rapidly as the solidification progresses and the process becomes conduction dominated. The same result is reported by Khodadadi and Hosseinizadeh [7] that the nanoparticle-embedded PCM, compared with the based PCM, can have higher heat extraction rate during the solidification process due to its lower latent heat and higher thermal conductivity.

Table 2 gives the liquid fraction for the four cases for a melting or solidification period of 1000 s. Due to the increase in thermal conductivity of the nanoPCM, the charging or melting rate is increased by 3.5%, 2.3%, and 3.5% for paraffin wax with 2%, 5%, and 10% Al_2O_3, re-

Table 2. Liquid fraction

Process	Pure paraffin wax	Paraffin wax with 2% Al_2O_3	Paraffin wax with 5% Al_2O_3	Paraffin wax with 10% Al_2O_3
Melting	0.86	0.89	0.88	0.89
Solidification	0.57	0.41	0.40	0.38

spectively, while the discharging or solidification rate is increased by 28.1%, 29.8%, and 33.3% for paraffin wax with 2%, 5%, and 10% Al_2O_3, respectively, as compared to the simple paraffin wax case.

Amount of energy stored

The amount of energy stored during the melting process and retrieved during the solidification process for a period of 1000 s is presented in tab. 3. The net energy stored is greater by 12.3%, 10.6%, and 15.4% during melting process and by 25.6%, 31.8%, and 41.5 % during solidification process, respectively for 2%, 5%, and 10% alumina in paraffin wax. Owing to the faster melting or solidification rate, the net energy stored or retrieved is greater for nanoPCM than simple PCM. It should be noted that the maximum amount of energy that can be stored depends on the amount of the PCM material stored in a unit of fixed size for a given operating temperature range. Hence, in both melting and solidification processes, maximum amount energy can be stored in or retrieved out is less than that of a pure paraffin wax unit . Consequently, there is decrease in theoretical energy storage capacity by 2.9%, 16.2%, and 31.9% for paraffin wax with 2%, 5%, and 10% Al_2O_3, respectively.

Table 3. Energy stored or retrieved in 1000 s

Process	Pure paraffin wax	Paraffin wax with 2% Al_2O_3	Paraffin wax with 5% Al_2O_3	Paraffin wax with 10% Al_2O_3
Melting	185617.11 J	208502.23 J	205288.74 J	214219.35 J
Solidification	111281.93 J	139793.71 J	146708.17 J	157415.62 J

Conclusions

In the present work, a numerical investigation has been carried out to find out the performance enhancement of paraffin wax with nanoalumina (Al_2O_3) particles in comparison with simple paraffin wax in a concentric double pipe heat exchanger. Numerical cyclic analysis indicates that the charge-discharge rates of thermal energy can be greatly enhanced using nanoPCM, as compared with a simple PCM. Embedding alumina particles in the paraffin wax enhances its low thermal conductivity and thus heat transfer rate. But the heat transfer rate enhancement is much more pronounced in conduction dominated solidification process than in natural convection dominated melting process. Further, lower volumetric concentration of alumina in paraffin wax not only exhibits good melting and solidification performance but also have high energy storage capacity and less cost compared to higher concentrations. Given stable suspension of nanoparticles within conventional phase change material such as paraffin wax, nanoPCM have great potential for greater utilization in diverse energy sectors.

Acknowledgment

The author, Dr. A. Valan Arasu gratefully acknowledges the financial support of the Department of Science and Technology, New Delhi, India, in the form of BOYSCAST Fellowship.

Nomenclature

A_{mush} – mushy zone constant
B – Boltzmann constant, [JK^{-1}]
c_p – specific heat capacity at constant pressure, [$Jkg^{-1}K^{-1}$]

d – diameter of nanoparticle, [mm]
g – gravitational acceleration, [ms^{-2}]
H – enthalpy of the nanoPCM, [Jkg^{-1}]
h – sensible enthalpy, [Jkg^{-1}]
K – thermal conductivity of nanoPCM, [Wm^{-1}K^{-1}]
L – latent heat of PCM, [Jkg^{-1}]
L_p – length of the PCM pipe, [m]
m – mass of PCM, [kg]
P – static pressure, [Nm^{-2}]
r_i – inner radius of the PCM pipe, [m]
r_o – outer radius of the PCM pipe, [m]
T – temperature of nanoPCM, [K]
$T_{liquidus}$ – liquidus temperature, [K]
T_m – melting or fusion temperature, [K]
T_{max} – maximum temperature, [K]
T_{min} – minimum temperature, [K]
$T_{solidus}$ – solidus temperature, [K]
T_{ref} – reference temperature
t – time, [s]
$\vec{U}$ – velocity, [ms^{-1}]

Greek symbols

β – liquid fraction
μ – dynamic viscosity, [Nsm^{-2}]
ρ – density, [kgm^{-3}]
$\boldsymbol{\tau}$ – stress tensor
ϕ – volumetric fraction of nanoparticle
ζ – correction factor

Subscripts

l – liquid PCM
np – nanoparticle
npcm – nanoPCM
s – solid PCM
pcm – base PCM

Reference

[1] Ismail, K. A. R., Goncalves, M. M., Analysis of a Latent Heat Cold Storage Unit, *Int. Journal of Energy Research, 21* (1997), 13, pp. 1223-1239
[2] Sharma, A., *et al*., Review on Thermal Energy Storage with Phase Change Materials and Applications, *Renewable and Sustainable Energy Reviews, 13* (2009), 2, pp. 318-345
[3] Lacroix, M., Study of the Heat Transfer Behavior of a Latent Heat Thermal Energy Storage Unit with a Finned Tube, *International, Journal of Heat Mass Transfer, 36* (1993), 8, pp. 2083-2092
[4] Vyashak, N. R., Jilani, G., Numerical Analysis of Latent Heat Thermal Energy Storage System, *Energy Conversion and Management, 48* (2007), pp. 2161-2168
[5] Cabeza, L. F., *et al*., Heat Transfer Enhancement in Water when Used as PCM in Thermal Energy Storage, *Applied Thermal Engineering, 22* (2002), 10, pp. 1141-1151
[6] Mettawee, E. S., Assassa, G. M. R., Thermal Conductivity Enhancement in a Latent Heat Storage System, *Solar Energy, 81* (2007), 7, pp. 839-845
[7] Khodadadi, J. M., Hosseinizadeh, S. F., Nanoparticle-Enhanced Phase Change Materials (NEPCM) with Great Potential for Improved Thermal Energy Storage, *International Communication in Heat Mass Transfer, 34* (2007), 5, pp. 534-543
[8] Zeng, J. L., *et al*., Study of a PCM Based Energy Storage System Containing Ag Nanoparticles, *Journal of Thermal Analysis Calorimetry, 87* (2007), 2, pp. 369-373
[9] Pincemin, S., *et al*., Elaboration of Conductive Thermal Storage Composites Made of Phase Change Materials and Graphite for Solar Power Plant, *ASME Journal of Solar Energy Engineering, 130* (2008), 1, pp. 11005-11009
[10] Kim, S., Drzal, L.T., High Latent Heat Storage and High Thermal Conductive Phase Change Materials Using Exfoliated Graphite Nanoplatelets, *Solar Energy Materials and Solar Cells, 93* (2009), 1, pp. 136-142
[11] Wang, X.Q., Mujumdar, A. S., Heat Transfer Characteristics of Nanofluids – A Review, *International Journal of Thermal Sciences, 46* (2007), 1, pp. 1-19
[12] Ho, C. J., Gao, T. Y., Preparation and Thermophysical Properties of Nanoparticle-In-Paraffin Emulsion as Phase Change Material, *International Communications in Heat and Mass Transfer, 36* (2009), 5, pp. 467-470
[13] Gong, Z. X., Mujumdar, A. S., A New Solar Receiver Thermal Store for Space-Based Activities Using Multiple Composite Phase Change Materials, *ASME Journal of Solar Energy Engineering, 117* (1995), 3, pp. 215-220
[14] Gong, Z. X., Mujumdar, A.S., Cyclic Heat Transfer in a Novel Storage Unit of Multiple Phase Change Materials, *Applied Thermal Engineering, 16* (1996), 10, pp. 807-815
[15] Gong, Z. X., Mujumdar, A.S., Enhancement of Energy Charge-Discharge Rates in Composite Slabs of Different Phase Change Materials, *International Journal of Heat and Mass Transfer, 39* (1996), 4, pp. 725-733

[16] Gong, Z. X., Mujumdar, A.S., Thermodynamic Optimization of the Thermal Process in Energy Storage Using Multiple Phase Change Materials, *Applied Thermal Engineering, 17* (1997), 11, pp. 1067-1083
[17] Hasan, M., *et al*., Cyclic Melting and Freezing, *Chemical Engineering Science, 46* (1991), 7, pp. 1573-1587
[18] ***, http://www.fluent.com.
[19] Kandasamy, R., *et al*., Transient Cooling of Electronics Using Phase Change Material (PCM)-Based Heat Sinks, *Applied Thermal Engineering, 28* (2008), 8-9, pp. 1047-1057
[20] Sasmito, A. P., *et al*., Numerical Evaluation of Laminar Heat Transfer Enhancement in Nanofluid Flow in Coiled Square Tubes, *Nanoscale Research Letters, 6* (2011), 1, p. 376
[21] Chow, L.C., Zhong, J.K., Thermal Conductivity Enhancement for Phase Change Storage Media, *International Communications in Heat and Mass Transfer, 23* (1996), 1, pp. 91-100
[22] Vajjha, R. S., *et al.*, Numerical Study of Fluid Dynamic and Heat Transfer Performance of Al_2O_3 and CuO Nanofluids in the Flat Tubes of a Radiator, *International Journal of Heat Fluid Flow, 31* (2010), 4, pp. 613-621

Paper submitted: April 17, 2011
Paper revised: November 30, 2011
Paper accepted: December 21, 2011